Aramwit et al. Nanoscale Research Letters 2014, 9:79
http://www.nanoscalereslett.com/content/9/1/79

Nanoscale Research Letters
a SpringerOpen Journal

NANO EXPRESS Open Access

Green synthesis of silk sericin-capped silver nanoparticles and their potent anti-bacterial activity

Pornanong Aramwit[1*], Nipaporn Bang[1], Juthamas Ratanavaraporn[2] and Sanong Ekgasit[3]

Abstract

In this study, a 'green chemistry' approach was introduced to synthesize silk sericin (SS)-capped silver nanoparticles (AgNPs) under an alkaline condition (pH 11) using SS as a reducing and stabilizing agent instead of toxic chemicals. The SS-capped AgNPs were successfully synthesized at various concentrations of SS and $AgNO_3$, but the yields were different. A higher yield of SS-capped AgNPs was obtained when the concentrations of SS and $AgNO_3$ were increased. The SS-capped AgNPs showed a round shape and uniform size with diameter at around 48 to 117 nm. The Fourier transform infrared (FT-IR) spectroscopy result proved that the carboxylate groups obtained from alkaline degradation of SS would be a reducing agent for the generation of AgNPs while COO^- and $NH_2{}^+$ groups stabilized the AgNPs and prevented their precipitation or aggregation. Furthermore, the SS-capped AgNPs showed potent anti-bacterial activity against various gram-positive bacteria (minimal inhibitory concentration (MIC) 0.008 mM) and gram-negative bacteria (MIC ranging from 0.001 to 0.004 mM). Therefore, the SS-capped AgNPs would be a safe candidate for anti-bacterial applications.

Keywords: Green synthesis; Silver nanoparticle; Silk sericin; Alkaline degradation; Anti-bacterial activity

Background

Over the last decades, silver nanoparticles (AgNPs) have been widely used in catalytic, optic, electronic, and other applications due to their unique size-dependent properties and high surface-to-volume ratio, which are significantly different from those of the corresponding bulk materials [1]. Recently, there has been a great deal of interest in the effective anti-bacterial/anti-fungal activity of AgNPs [2-5]. In fact, it is well known that Ag ions (Ag^+) and Ag-based compounds have strong biocidal effects on as many as 12 species of bacteria including *Escherichia coli* [6]. Das et al. showed that AgNPs with a 12-nm size could be used as effective growth inhibitors against *Bacillus subtilis*, *Staphylococcus aureus*, and *Pseudomonas aeruginosa* [3]. Kim et al. reported that yeast and *E. coli* were inhibited at the low concentration of AgNPs [7]. Furthermore, silver exhibits low toxicity and minimal risk in the human body [8].

AgNPs can be synthesized by a variety of methods such as reverse micelle process [9], chemical reduction [10], microwave dielectric heating reduction [11], ultrasonic irradiation [12], radiolysis [13], solvothermal synthesis [14], electrochemical synthesis [15], bacterial synthesis [16], etc. Among these methods, chemical reduction is one of the easiest and widely used techniques. Solomon et al. have reported the chemical reduction of silver nitrate using sodium borohydride to synthesize stable and non-aggregated AgNPs [17]. Sodium dodecyl sulfate, sodium citrate, and hydrazine hydrate solution were also used as stabilizing and reducing agents to prepare AgNPs with high anti-microbial activity against gram-positive bacteria [18]. However, these chemical methods use organic solvents and toxic reducing agents, consume high energy, and require difficult waste treatment. Recently, researchers have an increasing awareness about the environment. The use of toxic chemicals and solvents should be avoided, contributing to the emergence of 'green chemistry' for the synthesis of AgNPs [19-23]. Utilizations of

* Correspondence: aramwit@gmail.com
[1]Bioactive Resources for Innovative Clinical Applications Research Unit and Department of Pharmacy Practice, Faculty of Pharmaceutical Sciences, Chulalongkorn University, 254 PhyaThai Road, Patumwan, Bangkok 10330, Thailand
Full list of author information is available at the end of the article

Springer
© 2014 Aramwit et al.; licensee Springer. This is an Open Access article distributed under the terms of the Creative Commons Attribution License (http://creativecommons.org/licenses/by/2.0), which permits unrestricted use, distribution, and reproduction in any medium, provided the original work is properly credited.

environmentally friendly or naturally derived materials are some of the key issues of a green synthesis strategy [19-23]. Various types of microorganisms have been reported to synthesize AgNPs either intra- or extracellularly [19,20]. Also, stable AgNPs could be synthesized by using polysaccharides such as starch as both reducing and stabilizing agents [21,22]. AgNPs were synthesized by autoclaving a solution of $AgNO_3$ and starch [21]. Starch undergoes hydrothermal hydrolysis in an autoclave to produce glucose. Thus, starch can be used instead of pure glucose for the synthesis of AgNPs. In addition to polysaccharides, proteins, which are naturally abundant non-toxic materials and available from various sources, are introduced for AgNP synthesis. Zhao et al. have synthesized a AgNP-embedded soy protein isolation (SPI) film [24]. The whole reaction process was carried out by exposure to white light at ambient temperature, which is highly energy-efficient and eco-friendly. Moreover, the AgNP-embedded SPI film showed an effective antimicrobial activity against both gram-positive and gram-negative bacteria. Sasikala et al. have introduced the capabilities of the miracle bean soybean *Glycine max* as a stabilizer in the production of AgNPs [25]. Irwin et al. reported that keratin-stabilized AgNPs at 0.3 to 3 μM completely inhibited the growth of an equivalent volume of *ca.* 10^3 to 10^4 colony-forming units per milliliter (CFU/mL) of *S. aureus*, *Salmonella typhimurium*, or *E. coli* [26].

In this study, silk sericin protein was introduced for AgNP synthesis. Silk sericin (SS) is a water-soluble protein extracted from silkworms. Currently, SS is considered as a waste product from the textile industry. It is highly hydrophilic with strong polar side chains such as hydroxyl, carboxyl, and amino groups. Recently, SS has been widely used in biomaterial applications due to its biocompatibility, biodegradability, and anti-oxidative and bioactive activities. We herein introduced SS as a reducing and stabilizing agent for AgNP synthesis. Due to the results, SS can be used instead of other natural products to easily produce AgNPs. The effects of reaction conditions including the pH value and concentrations of SS and silver nitrate ($AgNO_3$) solutions on AgNP formation were investigated via a UV-visible (UV-Vis) spectrophotometer, transmission electron microscope (TEM), and colorimeter. The size and zeta potential of the SS-capped AgNPs were determined by using Zetasizer. The chemical structure of the SS-capped AgNPs was analyzed by attenuated total reflection Fourier transform infrared (ATR FT-IR) spectroscopy. The antimicrobial activity of the SS-capped AgNPs against gram-positive and gram-negative bacteria was evaluated.

Methods

Materials

Fresh bivoltine white-shell cocoons of *Bombyx mori* produced in a controlled environment were kindly supplied by Chul Thai Silk Co., Ltd. (Petchaboon province, Thailand). Silver nitrate ($AgNO_3$), sodium hydroxide (NaOH), and other chemicals were of analytical grade and used without further purification.

Preparation of silk sericin solution

The silkworm cocoons were cut into small pieces, and SS was extracted using a high-temperature and high-pressure degumming technique [27]. Briefly, the cocoons were put into deionized (DI) water and then autoclaved at 120°C for 60 min. After filtration through a filter paper to remove fibroin fibers, the SS solution was concentrated until the desired concentration was achieved (approximately 7 wt%, measured by the BCA protein assay kit, Pierce, Rockford, IL, USA). This SS solution was used as a stock solution. The molecular weight of the SS obtained ranged from 25 to 150 kDa, as reported previously [28].

Synthesis of SS-capped AgNPs

The SS solution was diluted to 5, 10, and 20 mg/mL, and NaOH was added to adjust the pH of the SS solution to be 9 and 11. The prepared SS solution was added to the $AgNO_3$ solution (1, 5, and 10 mM) under constant stirring. The mixture was stirred at room temperature overnight. The transparent solution which turned yellow indicated the formation of SS-capped AgNPs.

Characterization of SS-capped AgNPs

UV-Vis absorption spectra of the SS-capped AgNPs were measured using a UV-Vis spectrophotometer (Perkin-Elmer LAMBDA 25, Waltham, MA, USA), from 300 to 600 nm, to evaluate the formation and yield of SS-capped AgNPs. For the stability test, the SS-capped AgNP suspension was stored at different temperatures (4°C, 25°C, and 37°C) and the yield was analyzed at each pre-determined time. The concentrations of formed AgNPs were obtained from the calibration method. To construct the calibration curve, AgNP colloid standards at various initial $AgNO_3$ concentrations were prepared by reducing $AgNO_3$ with $NaBH_4$ in the SS solution. The amount of $NaBH_4$ used in the reaction was excessive, and the dissolved silver ions completely transformed into metallic silver. The characteristic plasmon absorption at 420 nm was plotted against the initial concentration of $AgNO_3$ and employed as a calibration curve. The plasmon absorption intensity at 420 nm directly related to the amount of AgNPs formed. The color of the SS-capped AgNP suspension was determined using a colorimeter (Konica Minolta CR 400, Chiyoda-ku, Japan). The CIELab scale was used; lightness (L^*) and chromaticity parameter b^* (yellow-blue) were measured. The size and zeta potential of SS-capped AgNPs were determined by Zetasizer Nano Range (Malvern Instruments Ltd, Malvern, UK). A drop of SS-capped AgNPs was placed on carbon-coated

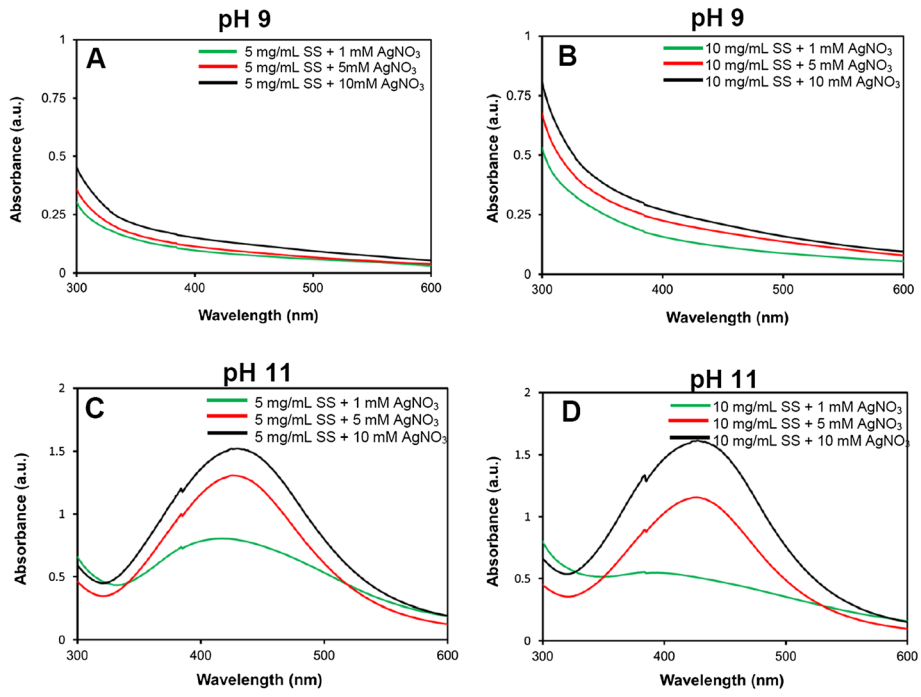

Figure 1 Formation of SS-capped AgNPs at pH 9 and 11. (A) 5 mg/mL SS + 1, 5, 10 mM $AgNO_3$ at pH 9, **(B)** 10 mg/mL SS + 1, 5, 10 mM $AgNO_3$ at pH 9, **(C)** 5 mg/mL SS + 1, 5, 10 mM $AgNO_3$ at pH 11, **(D)** 10 mg/mL SS + 1, 5, 10 mM $AgNO_3$ at pH 11.

copper grids and observed on TEM (Hitachi H-7650, Chiyoda-ku, Japan).

The chemical structure of the SS-capped AgNPs was analyzed by ATR FT-IR spectroscopy. Briefly, the SS-capped AgNP suspension was dropped on a glass slide and left to dry overnight under an ambient condition. The ATR spectrum was collected by a germanium micro-internal reflective element (IRE) attached onto the built-in × 15 infrared objective. A sufficient contact between the tip of the IRE and the sample was achieved by raising the sample stage towards the IRE. The degree of contact was monitored by a built-in pressure sensor on the sample stage. The ATR spectra were collected via a continuum infrared microscope attached to a Nicolet 6700 FT-IR spectrometer (Thermo Fisher Scientific, Waltham, MA, USA) using a 256-scan co-addition at a resolution of 4 cm^{-1} with a built-in nitrogen-cooled mercury-cadmium-telluride (MCT) detector.

Evaluation of anti-bacterial activities of SS-capped AgNPs

All bacterial experiments were performed in a laminar flow hood according to the full aseptic technique protocol. The researchers wore a cap, a mask, and gloves during the experiment to prevent the contamination of harmful bacteria. The anti-bacterial activities of SS-capped AgNPs were analyzed by broth dilution method against six different pathogenic microorganisms including gram-positive bacteria (*Bacillus subtilis*, *S. aureus*, and methicillin-resistant *S. aureus* (MRSA)) and gram-negative bacteria (*E. coli*, *P. aeruginosa*, and *Acinetobacter baumannii*). The pure cultures of bacteria were subcultured on Mueller-Hinton agar (MHA). Each strain was inoculated into soybean casein digest (tryptic soy broth (TSB)) for 4 to 6 h at 37°C. The growth cultures were diluted to 5×10^5 CFU/mL. AgNP suspension (1 mL) was added to the mixture of TSB (1 mL) and the bacterial culture (1 mL). After incubation at 37°C for 24 h, the

Table 1 Yield, size, and zeta potential of SS-capped AgNPs synthesized from SS and $AgNO_3$ at pH 11

Sample	Yield of AgNPs (mM)	Size (nm)	Zeta potential (mV)
5 mg/mL SS + 1 mM $AgNO_3$	0.06	95.8 ± 0.9	−23.7 ± 0.6
5 mg/mL SS + 5 mM $AgNO_3$	0.75	48.8 ± 0.1*	−25.2 ± 0.2
5 mg/mL SS + 10 mM $AgNO_3$	0.88	55.2 ± 0.6*	−17.1 ± 0.6
10 mg/mL SS + 1 mM $AgNO_3$	0.04	117.0 ± 6.8	−22.0 ± 0.1
10 mg/mL SS + 5 mM $AgNO_3$	0.66	48.1 ± 0.2*	−25.5 ± 0.9
10 mg/mL SS + 10 mM $AgNO_3$	0.93	63.6 ± 1.6*	−18.8 ± 2.3

*$p < 0.05$, significant against the values of SS-capped AgNPs synthesized from 1 mM $AgNO_3$ at the corresponding SS concentration.

minimal inhibitory concentration (MIC) was examined. It is expressed as the lowest dilution which inhibited growth, judged by the lack of turbidity in the tube. After the bacterial experiment, the used cap, mask, and gloves were autoclaved before disposal. The flasks were autoclaved for sterilization, and the area was disinfected with 70% ethanol.

Statistical analysis

All the results were statistically analyzed by the unpaired Student's t test, and $p < 0.05$ was considered to be statistically significant. Data were expressed as the mean ± standard deviation.

Results and discussion

In this work, SS was selected as a reducing and a stabilizing agent for the synthesis of AgNPs under an alkaline condition due to its being environmentally friendly, biocompatibility, and functional groups with reducing potential. The effects of pH and concentrations of $AgNO_3$ and SS on the formation of SS-capped AgNPs are shown in Figure 1. It was found that the SS-capped AgNPs could not be formed at pH 9 at any concentration of SS and $AgNO_3$. On the other hand, at pH 11, all concentrations of SS (5 and 10 mg/mL) and $AgNO_3$ (1, 5, and 10 mM) formed SS-capped AgNPs with different yields. This is because the functional groups with reducing potential of SS could be obtained from the alkaline degradation [29-31]. SS is a hydrophilic protein with strong polar side chains such as hydroxyl, carboxyl, and amino groups. It was supposed that the SS degraded under strong alkaline condition would generate the reducing species that could reduce silver ions [21]. Furthermore, the abundant hydroxyl groups of SS were expected to complex with the silver ion and prevent aggregation or precipitation of AgNPs [21,32]. The effect of the acidic-alkaline treatment of soluble starch on the synthesis of metal nanoparticles was reported by Tongsakul et al. [29]. They found that degraded intermediates with reducing potential (i.e., aldehyde and α-hydroxy ketone) of starch are concomitantly generated when the alkaline concentration is greater than 0.025 M and the *in situ* generated species could completely reduce platinum ions (20 mM) and sufficiently stabilize the obtained platinum nanoparticles (5 mM) of uniform particle size (2 to 4 nm).

Table 2 Color quantitative results of SS-capped AgNP suspension synthesized from SS and $AgNO_3$ at pH 11

Sample	L^*	b^*
5 mg/mL SS + 5 mM $AgNO_3$	17.7 ± 0.0	0.3 ± 0.0
10 mg/mL SS + 5 mM $AgNO_3$	17.7 ± 0.4	0.4 ± 0.1

L^* indicates brightness ranging from black ($L^* = 0$) to white ($L^* = 100$). b^* indicates blue-yellow color, value ranged from −60 (blue) to 60 (yellow).

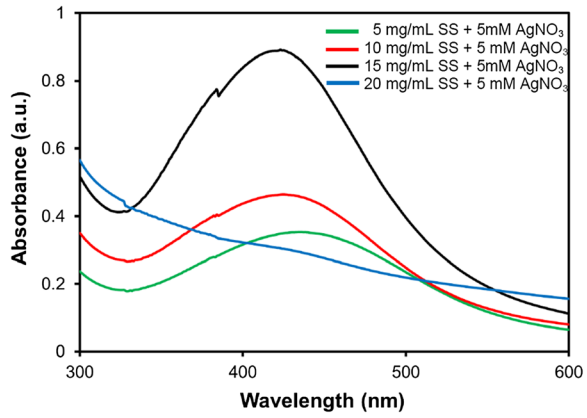

Figure 2 Formation of SS-capped AgNPs synthesized from SS and $AgNO_3$ at pH 11.

The SS-capped AgNPs had a yellow-brown color with a typical absorption peak of AgNPs at 420 nm [21]. The yield of SS-capped AgNPs increased with the increasing concentration of $AgNO_3$. However, the concentration of SS seemed to show less effect on the yield of SS-capped AgNPs. Yields of SS-capped AgNPs synthesized at pH 11 are presented in Table 1. It was clearly seen that the yields of SS-capped AgNPs synthesized from 10 mg/mL SS + 1 mM $AgNO_3$ were the lowest (0.04 mM) while those synthesized from 10 mg/mL SS + 10 mM $AgNO_3$ were the highest (0.93 mM) according to the absorption intensity and AgNP concentration standard curve. At both 5 and 10 mg/mL SS, $AgNO_3$ at 5 and 10 mM produced 0.66 to 0.93 mM SS-capped AgNPs. The colors of the AgNP suspension were quantitatively evaluated as presented in Table 2. L^* and b^* indicated the lightness and yellow-blue color of the suspension, respectively. The AgNP suspensions synthesized from 5 or 10 mg/mL SS + 1 mM $AgNO_3$ were lighter (higher L^* values) and more likely yellow (higher b^* values) than those synthesized from 5 or 10 mg/mL SS + 5 mM $AgNO_3$. The lighter color of the AgNP suspension indicated a lower yield of SS-capped AgNPs than the darker (brown) suspension. Thus, the higher concentration of $AgNO_3$ produced the higher yield of SS-capped AgNPs.

The effects of the wider range of SS concentration (5, 10, 15, and 20 mg/mL) at a fixed concentration of $AgNO_3$ (5 mM) on the formation of SS-capped AgNPs were

Table 3 Yield of SS-capped AgNPs synthesized from SS and $AgNO_3$ at pH 11

Sample	Yield of AgNPs (mM)
5 mg/mL SS + 5 mM $AgNO_3$	0.47
10 mg/mL SS + 5 mM $AgNO_3$	0.63
15 mg/mL SS + 5 mM $AgNO_3$	1.26
20 mg/mL SS + 5 mM $AgNO_3$	-

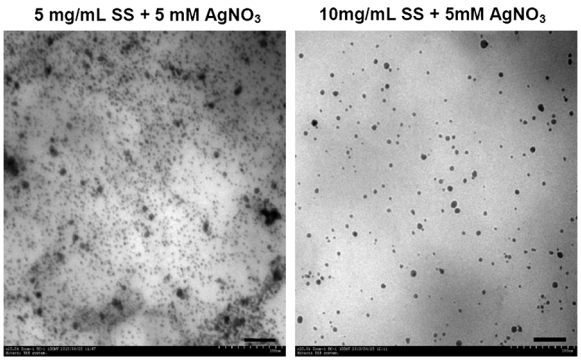

Figure 3 Morphology of SS-capped AgNPs synthesized from SS and $AgNO_3$ at pH 11, observed on TEM. Scale bar = 1 μm.

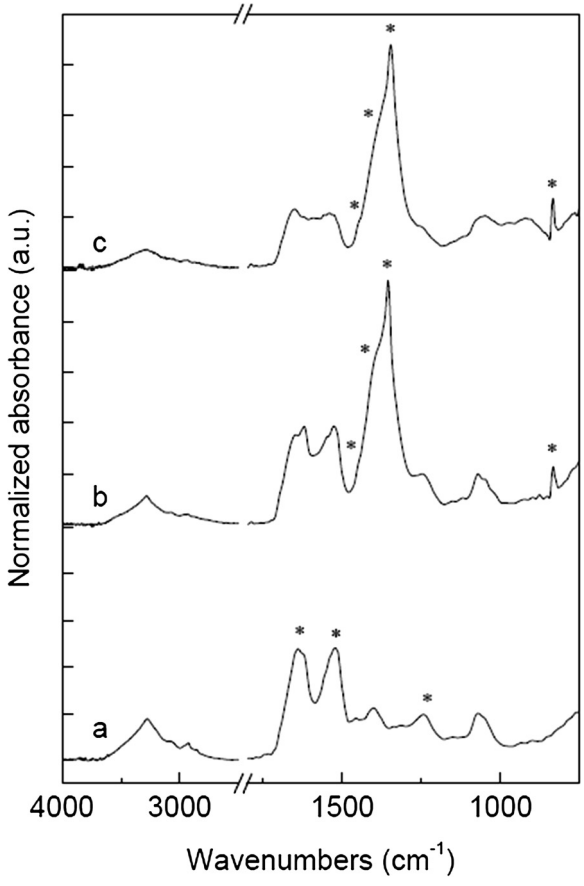

Figure 4 Normalized ATR FT-IR spectra of virgin sericin and AgNPs. The intensity was normalized against the absorption at 1,070 cm^{-1}. **(A)** Original SS shows characteristic absorptions of protein including amide I (1,700 to 1,600 cm^{-1}, asterisk), amide II (1,560 to 1,500 cm^{-1}, asterisk), and amide III (1,300 to 1,200 cm^{-1}, asterisk). **(B)** SS-capped AgNPs show new functional groups including carboxylate (1,451, 1,404, 1,353 cm^{-1}, asterisk) and amine salt (830 cm^{-1}, asterisk). **(C)** Thermally treated SS-capped AgNPs show the same functional groups as those in **(B)**.

Table 4 Infrared band assignment of silk sericin and SS-capped AgNPs

IR band (cm^{-1})	Band assignment
1,700 to 1,600	Amide I (C = O stretching vibration)
1,560 to 1,500	Amide II (N-H bending and C-N stretching vibration)
1,300 to 1,200	Amide III (C-N-H in-plane bending and C-N stretching vibration)
1,451, 1,404, 1,353	Free carboxylate groups (COO^- stretching vibration)
830	Amine salt

further investigated, as shown in Figure 2. It was found that 5, 10, and 15 mg/mL of SS + 5 mM of $AgNO_3$ could produce SS-capped AgNPs and the yield increased with the increasing concentration of SS (0.47, 0.63, and 1.26 mM, respectively), as presented in Table 3. Interestingly, at 20 mg/mL of SS, the peak absorption at 420 nm was not observed. The mechanism of this phenomenon was not clearly understood at present. It was supposed that the high SS concentration provided excessive stabilization of Ag^+. As a result, Ag^+ was slowly reduced. An increase in the absorption at 420 nm or intense yellow color over time was observed.

Sizes and zeta potentials of SS-capped AgNPs synthesized at pH 11 are presented in Table 1. The SS-capped AgNPs synthesized from 5 or 10 mg/mL SS + 1 mM $AgNO_3$ showed the largest size (95.8 and 117 nm, respectively). When the concentration of $AgNO_3$ was increased to 5 or 10 mM, SS-capped AgNPs with smaller size (48 to 63 nm) were formed. However, it seemed that sizes of all nanoparticles were in a similar range (48 to 117 nm). TEM images in Figure 3 qualitatively show the round shape of SS-capped AgNPs and confirm their size

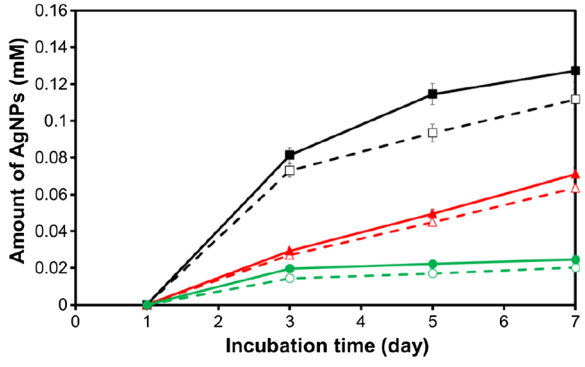

Figure 5 Stability of SS-capped AgNPs synthesized at pH 11 when stored at different temperatures. (empty square) 5 mg/mL SS + 5 mM $AgNO_3$, 37°C, (filled square) 10 mg/mL SS + 5 mM $AgNO_3$, 37°C, (empty triangle) 5 mg/mL SS + 5 mM $AgNO_3$, 25°C, (filled triangle) 10 mg/mL SS + 5 mM $AgNO_3$, 25°C, (empty circle) 5 mg/mL SS + 5 mM $AgNO_3$, 4°C, (filled circle) 10 mg/mL SS + 5 mM $AgNO_3$, 4°C.

Table 5 Anti-bacterial activity of SS-capped AgNPs (5 mg/mL SS + 5 mM $AgNO_3$) against gram-positive and gram-negative bacteria

Gram	Bacterial strain	Concentration of SS-capped AgNPs (mM)					MIC (mM)
		0.001	0.004	0.008	0.017	0.034	
+	MRSA	T	T/C	C	C	C	0.008
+	*S. aureus*	T	T/C	C	C	C	0.008
+	*B. subtilis*	T	T/C	C	C	C	0.008
–	*P. aeruginosa*	T	C	C	C	C	0.004
–	*A. baumannii*	C	C	C	C	C	0.001
–	*E. coli*	T	C	C	C	C	0.004

T, turbid suspension; T/C, slightly turbid suspension; C, clear solution.

as reported in Table 1. Zeta potentials of all SS-capped AgNPs were around −25 to −17 mV, indicating their high stability.

Figure 4 and Table 4 show the normalized ATR FT-IR spectra and infrared band assignment of the original SS and SS-capped AgNPs. The spectrum of the original SS (Figure 4(A)) showed characteristic absorptions of protein including amide I (1,700 to 1,600 cm^{-1}), amide II (1,560 to 1,500 cm^{-1}), and amide III (1,300 to 1,200 cm^{-1}) [33]. After the addition of silver salt under an alkaline condition (Figure 4(B)), an obvious presence of new functional groups including carboxylate (1,451, 1,404, 1,353 cm^{-1}) and amine salt (830 cm^{-1}) was observed. The new absorptions indicated the hydrolysis of amide linkage into its basic structural units [34]. The carboxylate groups also function as a weak reducing agent for the generation of AgNPs [35-38]. This FT-IR data proved the mechanism of how SS under an alkaline condition formed the AgNPs. In addition, the reduction reaction was accelerated by the thermal treatment of the SS-capped AgNPs (Figure 4(C)). The carboxylate (COO^-) and amine ($NH_2{}^+$) moieties were clearly present. It was reported that these moieties could stabilize AgNPs through the donated lone pair electrons to the surface of metal nanoparticles [35,38]. An excellent stabilization of AgNPs by COO^- and NH_2^+ groups also prevented precipitation and aggregation of the nanoparticles [21,32].

The synthesized SS-capped AgNPs were stored at different temperatures (4°C, 25°C, and 37°C) for 7 days to observe their stability, as shown in Figure 5. It was found that the SS-capped AgNPs stored at 4°C were rather stable along the 7-day period; on the other hand, more SS-capped AgNPs were formed when stored at 25°C and 37°C. This might be that the reduction reaction continued at higher temperature.

The anti-bacterial activity of SS-capped AgNPs against gram-positive and gram-negative bacteria is shown in Table 5. The SS-capped AgNPs synthesized from 5 mg/mL SS + 5 mM $AgNO_3$ were selected for the study due to their high yield and stability. We found that the growth of all gram-positive bacteria (MRSA, *S. aureus*, and *B. subtilis)* was potentially inhibited by SS-capped AgNPs (MIC 0.008 mM) while the SS-capped AgNPs inhibited the growth of gram-negative bacteria at a lower MIC (0.004 mM for *P. aeruginosa* and *E. coli* and 0.001 mM for *A. baumannii*). This result clearly elucidated the effectiveness of our SS-capped AgNPs for anti-bacterial applications.

Conclusions

SS-capped AgNPs were successfully synthesized under an alkaline condition (pH 11) via a green chemistry approach using SS as a reducing and stabilizing agent. The higher concentrations of SS and $AgNO_3$ increased the yield of SS-capped AgNPs. Sizes of the SS-capped AgNPs were around 48 to 117 nm. The FT-IR result proved that the carboxylate groups obtained from alkaline degradation of SS would be a reducing agent for the generation of AgNPs while COO^- and NH_2^+ groups stabilized the AgNPs and prevented their precipitation or aggregation. Furthermore, the SS-capped AgNPs showed potent anti-bacterial activity against various gram-positive and gram-negative bacteria. We therefore introduced the SS-capped AgNPs as a safe candidate for anti-bacterial applications.

Competing interests

The authors declare that they have no competing interests.

Authors' contributions

PA designed all the experiments and interpreted and discussed all the results. NB did the microbiology study. JR drafted the manuscript. TT performed some parts of the experiments. SE ran the FT-IR experiment. All authors read and approved the final manuscript.

Acknowledgements

This research was supported by Thailand Research Fund (TRF).

Author details

[1]Bioactive Resources for Innovative Clinical Applications Research Unit and Department of Pharmacy Practice, Faculty of Pharmaceutical Sciences, Chulalongkorn University, 254 PhyaThai Road, Patumwan, Bangkok 10330, Thailand. [2]Department of Chemical Engineering, Faculty of Engineering, Chulalongkorn University, 254 PhyaThai Road, Patumwan, Bangkok 10330, Thailand. [3]Sensor Research Unit, Department of Chemistry, Faculty of Science, Chulalongkorn University, 254 PhyaThai Road, Patumwan, Bangkok 10330, Thailand.

Received: 26 November 2013 Accepted: 10 February 2014
Published: 17 February 2014

References

1. Feldheim DL, Foss CA: *Metal Nanoparticles: Synthesis, Characterization and Applications.* New York: Marcel Dekker; 2002.
2. Lok CN, Ho CM, Chen R, He QY, Yu WY, Sun H, Tam PKH, Chiu JF, Che CM: **Proteomic analysis of the mode of antibacterial action of silver nanoparticles.** *J Proteome Res* 2006, **5:**916–924.
3. Das R, Gang S, Nath SS: **Preparation and antibacterial activity of silver nanoparticles.** *J Biomater Nanobiotechnol* 2011, **2:**472–475.
4. Li WR, Xie XB, Shi QS, Zeng HY, OU-Yang YS, Chen YB: **Antibacterial activity and mechanism of silver nanoparticles on *Escherichia coli*.** *Appl Microbiol Biotechnol* 2010, **85:**1115–1122.
5. Chao L, Xiansong W, Feng C, Chunlei Z, Xiao Z, Kan W, Xiangcui D: **The antifungal activity of graphene oxide–silver nanocomposites.** *Biomaterials* 2013, **34:**3882–3890.
6. Zhao G, Stevens SE Jr: **Multiple parameters for the comprehensive evaluation of the susceptibility of Escherichia coli to the silver ion.** *Biometals* 1998, **11:**27–32.
7. Kim JS, Kuk E, Yu KN, Kim JH, Park SJ, Lee HJ, Kim SH, Park YK, Park YH, Hwang CY, Kim YK, Lee YS, Jeong DH, Cho MH: **Antimicrobial effects of silver nanoparticles.** *Nanomedicine* 2007, **3:**95–101.
8. Lansdown AB: **Silver in health care: antimicrobial effects and safety in use.** *Curr Probl Dermatol* 2006, **33:**17–34.
9. Xie Y, Ye R, Liu H: **Synthesis of silver nanoparticles in reverse micelles stabilized by natural biosurfactant.** *Colloids Surfaces A* 2006, **279:**75–178.
10. Pillai ZS, Kamat PV: **What factors control the size and shape of silver nanoparticles in the citrate ion reduction method.** *J Phys Chem B* 2004, **108:**945–951.
11. Patel K, Kapoor S, Dave DP, Murherjee T: **Phenomenon is related to size of colloidal silver particles.** *J Chem Sci* 2005, **117:**53–60.
12. Salkar RA, Jeevanandam P, Aruna ST, Koltypin Y, Gedanken A: **The sonochemical preparation of amorphous silver nanoparticles.** *J Mater Chem* 1999, **9:**1333–1335.
13. Soroushian B, Lampre I, Belloni J, Mostafavi M: **Radiolysis of silver ion solutions in ethylene glycol: solvated electron and radical scavenging yields.** *Radiat Phys Chem* 2005, **72:**111–118.
14. Starowicz M, Stypula B, Banaœ J: **Electrochemical synthesis of silver nanoparticles.** *Electrochem Commun* 2006, **8:**227–230.
15. Zhu JJ, Liao XH, Zhao XN, Hen HY: **Preparation of silver nanorods by electrochemical methods.** *Mater Lett* 2001, **49:**91–95.
16. Thomas R, Viswan A, Mathew J, Radhakrishnan EK: **Evaluation of antibacterial activity of silver nanoparticles synthesized by a novel strain of marine Pseudomonas sp.** *Nano Biomed Eng* 2012, **4:**139–143.
17. Solomon SD, Bahadory M, Jeyarajasingam AV, Rutkowsky SA, Boritz C: **Synthesis and study of silver nanoparticles.** *J Chem Educ* 2007, **84:**322–325.
18. Guzmán MG, Dille J, Godet S: **Synthesis of silver nanoparticles by chemical reduction method and their antibacterial activity.** *Int J Chem Biol Eng* 2009, **2:**104–111.
19. Rani PU, Rajasekharreddy P: **Green synthesis of silver-protein (core–shell) nanoparticles using Piper betle L. leaf extract and its ecotoxicological studies on Daphnia magna.** *Colloids Surfaces A* 2011, **389:**188–194.
20. Li G, He D, Qian Y, Guan B, Gao S, Cui Y, Yokoyama K, Wang L: **Fungus-mediated green synthesis of silver nanoparticles using Aspergillus terreus.** *Int J Mol Sci* 2012, **13:**466–476.
21. Vigneshwaran N, Nachane RP, Balasubramanya RH, Varadarajan PV: **A novel one-pot 'green' synthesis of stable silver nanoparticles using soluble starch.** *Carbohyd Res* 2006, **341:**2012–2018.
22. Oluwafemi OS, Vuyelwa N, Scriba M, Songca SP: **Green controlled synthesis of monodispersed, stable and smaller sized starch-capped silver nanoparticles.** *Mater Lett* 2013, **106:**332–336.
23. Senthamilselvi S, Kumar P, Prabha AL, Govindaraju M: **Green simplistic biosynthesis of anti-bacterial silver nanoparticles using Annona squamosa leaf extract.** *Nano Biomed Eng* 2013, **5:**102–106.
24. Zhao S, Yao J, Fei X, Shao Z, Chen X: **An antimicrobial film by embedding in situ synthesized silver nanoparticles in soy protein isolate.** *Mater Lett* 2013, **95:**142–144.
25. Sasikala D, Govindaraju K, Tamilselvan S, Singaravelu G: **Soybean protein: a natural source for the production of green silver nanoparticles.** *Biotechnol Bioprocess Eng* 2012, **17:**1176–1181.
26. Irwin P, Martin J, Nguyen LH, He Y, Gehring A, Chen CY: **Antimicrobial activity of spherical silver nanoparticles prepared using a biocompatible macromolecular capping agent: evidence for induction of a greatly prolonged bacterial lag phase.** *J Nanobiotechnology* 2010, **8:**34.
27. Lee K, Kweon H, Yeo JH, Woo SO, Lee YW, Cho CS, Kim KH, Park YH: **Effect of methyl alcohol on the morphology and conformational characteristics of silk sericin.** *Int J Biol Macromol* 2003, **33:**75–80.
28. Aramwit P, Kanokpanont S, Nakpheng T, Srichana T: **The effect of sericin from various extraction methods on cell viability and collagen production.** *Int J Mol Sci* 2010, **11:**2200–2211.
29. Tongsakul D, Wongravee K, Thammacharoen C, Ekgasit S: **Enhancement of the reduction efficiency of soluble starch for platinum nanoparticles synthesis.** *Carbohyd Res* 2012, **357:**90–97.
30. Knill CJ, Kennedy JF: **Degradation of cellulose under alkaline conditions.** *Carbohydr Polym* 2003, **51:**281–300.
31. Clarke MA, Edye LA, Eggleston G: *Advances in Carbohydrate and Biochemistry.* San Diego: Academic; 1997:449–455.
32. Shin Y, Bae IT, Exarhos GJ: **Green approach for self-assembly of platinum nanoparticles into nanowires in aqueous glucose solutions.** *Colloids Surface A* 2009, **348:**191–195.
33. Khan MR, Tsukada M, Zhang X, Morikawa H: **Preparation and characterization of electrospun nanofibers based on silk sericin powders.** *J Mater Sci* 2013, **48:**3731–3736.
34. Socrates G: *Infrared and Raman Characteristic Group Frequencies: Table and Chart.* Chichester: Wiley; 2000.
35. Rafey A, Shrivastavaa KBL, Iqbal SA, Khan Z: **Growth of Ag-nanoparticles using aspartic acid in aqueous solutions.** *J Colloid Interf Sci* 2011, **354:**190–195.
36. Dong Q, Su H, Zhang D: **In situ depositing silver nanoclusters on silk fibroin fibers supports by a novel biotemplate redox technique at room temperature.** *J Phys Chem B* 2005, **109:**17429–17434.
37. Zhong Z, Patskovskyy S, Bouvrette P, Luong JHT, Gedanken A: **The surface chemistry of Au colloids and their interactions with functional amino acids.** *J Phys Chem B* 2004, **108:**4046–4052.
38. Song J, Roh J, Lee I, Jang J: **Low temperature aqueous phase synthesis of silver/silver chloride plasmonic nanoparticles as visible light photocatalysts.** *Dalton Trans* 2013, **42:**13897–13904.

doi:10.1186/1556-276X-9-79
Cite this article as: Aramwit *et al.*: Green synthesis of silk sericin-capped silver nanoparticles and their potent anti-bacterial activity. *Nanoscale Research Letters* 2014 **9**:79.

Submit your manuscript to a SpringerOpen journal and benefit from:

- ► Convenient online submission
- ► Rigorous peer review
- ► Immediate publication on acceptance
- ► Open access: articles freely available online
- ► High visibility within the field
- ► Retaining the copyright to your article

Submit your next manuscript at ► springeropen.com